Supporting Information for

In situ Formation of Gold Nanoparticles@Supramolecular Hydrogel with Ultra-fast Catalytic Reduction of Dyes and Excellent Anti-bacterial Property

Xiao-Juan Wang [a], Lang Zhang [a], Chuan-Wan Wei [a*], Shu-Qin Gao [b], Wei Luo [a], and Ying-Wu Lin [a,b*]

[a] School of Chemistry and Chemical Engineering, University of South China, Hengyang 421001, China; [b] Key Lab of Protein Structure and Function of Universities in Hunan Province, University of South China, Hengyang 421001, China.

Corresponding authors:
*E-mail: weichw@hotmail.com (C.-W. Wei); ywlin@usc.edu.cn (Y.-W. Lin)

Contents

L-tyrosine (L-Tyr) and Quinoline-2-formaldehyde, Gold chloride solution ($HAuCl_4$), sodium borohydride ($NaBH_4$), Methyl orange, 4-Nitrophenyl, Isatin, Amaranth, were purchased from Aladin Reagent (Shanghai, China). Reactive black 5, Reactive red 120, Reactive orange 16 were purchased from Sigma-Aldrich, Methylene blue was purchased from Damas-beta. Methyl green was purchased from Solarbio, which was used without further purification. *Bacilus subtilis* was purchased from HuanKai Microbial. All other reagents were of analytical grade, which include HCl, KOH, absolute alcohol etc. Deionized water (MillQ, 18.2 MΩ) was used.

1.2 Synthesis of 2-QY

Mixing an aqueous solution of L-tyrosine (5 mmol) containing potassium hydroxide (0.28 g, 5 mmol) and the ethanol solution of 2-quinolinecarboxaldehyde (5 mmol), and the mixture was stirred at 50 °C for 4 h and then cooled in an ice bath. Sodium borohydride (6 mmol) was slowly added to the solution and was stirred for another 5 h. Finally, the reaction mixture was neutralized with hydrochloric acid and the pH was adjusted about 7. The obtained crude product with pale yellow in color was washed with ethanol and water, and then was dried.

ESI-MS: Calc. for $C_{19}H_{18}N_2O_3$ 322.1 Da, observed 321.2 Da [M-H] (Fig.S1).

^{1}H NMR (500 MHz, D_2O) δ 8.18 (d, *J* = 8.5 Hz, 1H), 7.82 (d, *J* = 9.0 Hz, 2H) ,7.67 (t, *J* = 7.5 Hz, 1H), 7.49 (t, *J* = 7.5 Hz, 1H), 7.29 (d, *J* = 8.5 Hz, 1H), 6.81 (d, *J* = 8.5 Hz, 2H), 6.41 (d, *J* = 8.5 Hz, 2H), 3.89 (dd, *J* = 96,14.0 Hz, 2H), 3.18 (t, *J* = 6.5 Hz, 1H), 2.65 (ddd, 2H), 1.04 (t, *J* = 7.0 Hz, 1H) (Fig.S2).

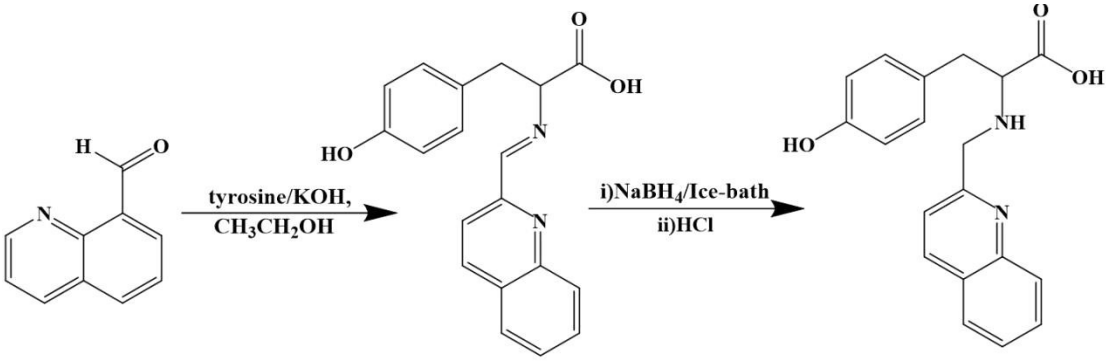

Scheme S1 The synthesis of 2-QY.

1.3 The preparation of 2-QY-Au NPs metallohydrogel

Adjusting the pH of 2-QY solution (0.03 M) to 10.3, and then addition of $HAuCl_4$ solution at the molar ratio of 1:1, the mixture changed from yellow to light green to dark brown when it was treated with sonication for 20 min. The above dark brown solution became purple 2-QY-Au NPs metallohydrogel after standing for about 5 h.

1.4 UV-Vis studies

UV-Vis spectral changes in reduction of various dyes by $NaBH_4$ in the presence of 2-QY-Au NPs metallohydrogel were recorded in deionized water on a Hewlett-Packard 8453 diode array spectrometer and a dual mixing stopped-flow spectrophotometer (SF-61DX2 Hi-Tech Kinet Asyst^{TM}). The experimental details were depicted under every absorption spectrum curve in the text and supporting information. The reaction rate was elevated using the apparent rate constant (k_{app}), which determined by equation (1) and (2). The catalytic efficiency was expressed in terms of Turnover number (TON) and turnover frequency (TOF), which was calculated by the equations (3) and (4).

$$\frac{dC_t}{dt} = -k_{app}C_t \qquad (1)$$

$$\ln\frac{C_t}{C_0} = \ln\frac{A_t}{A_0} = -k_{app}t \quad (2)$$

$$\text{TON} = \frac{\%\text{degradation} \times \text{number of moles of dye}}{\text{number of moles of catalyst}} \quad (3)$$

$$\text{TOF} = \frac{\%\text{degradation} \times \text{number of moles of dye}}{\text{number of moles of catalyst} \times \text{time}} \quad (4)$$

1.5 MTT study

MTT (3-(4,5)-dimethylthiahiazo(-z-y1)-3,5-di-phenytetrazoliumromide) colorimetric analysis was carried out on Hela cells to detect the cell toxicity of 2-QY and 2-QY-Au NPs metallohydrogel. The cells were inoculated in 96-well cell culture plate and they were incubated in an incubator for 24 h. Different concentrations of 2-QY and diluted 2-QY-Au NPs metallohydrogel (ranging from 0 to 300 μM) were then injected into the wells, and the cells were incubated at 37 ℃ for 24 h and 48 h, respectively. Three parallel experiments were conducted for each one. And then, they were observed by inverted microscopy. The MTT was added to the cells in 96-well plates, and continued to incubate for 4 h. The incubation was terminated and the medium was aspirated, during this period, the cells reacted with MTT solution to produce Formazan crystals. Lastly, 150 μL of DMSO was added to each well, and the cells were shaken at low speed for 10 min to fully dissolve the Formazan crystals. An enzyme-linked immunosorbent assay (ELISA) reader (infinite M200, Tecan, Aus-tria) was utilized to obtain the OD at 490 nm (absorbance value) of each well.

2. Supplementary Figures

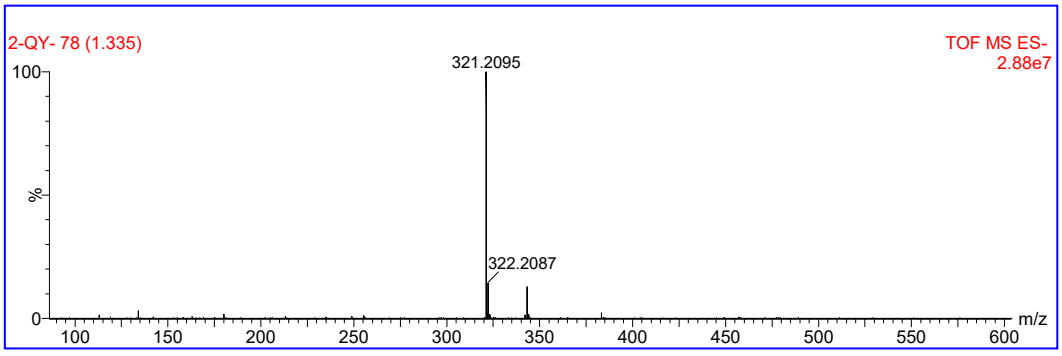

Fig. S1 ESI-MS spectra of 2-QY, Calculated: 322.3 Da; Observed: 321.2 Da ([2-QY -H]).

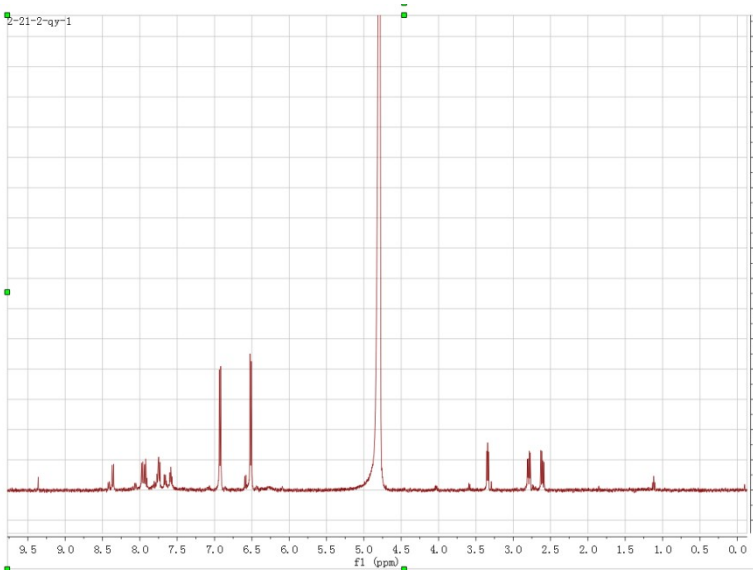

Fig. S2 ^{1}H NMR spectrum of the Schiff's base (precursor of 2-QY) in D_2O.

^{1}H NMR (500 MHz, D_2O) δ 9.36(s, 1H), 8.36(d, *J* = 9.0 Hz, 1H), 7.97(d, *J* = 9.0 Hz, 2H) ,7.92(t, *J* = 7.5 Hz, 1H), 7.49(t, *J* = 7.5 Hz, 1H), 7.59(d, *J* = 8.5 Hz, 1H), 6.92(d, *J* = 8.5 Hz, 2H), 6.51(d, *J* = 8.5 Hz, 2H), 3.41(dd, *J* = 5.0 Hz, 1H), 2.79(dd, *J* = 5.0 Hz,1H), 2.61(dd, *J* = 5.0 Hz,1H).

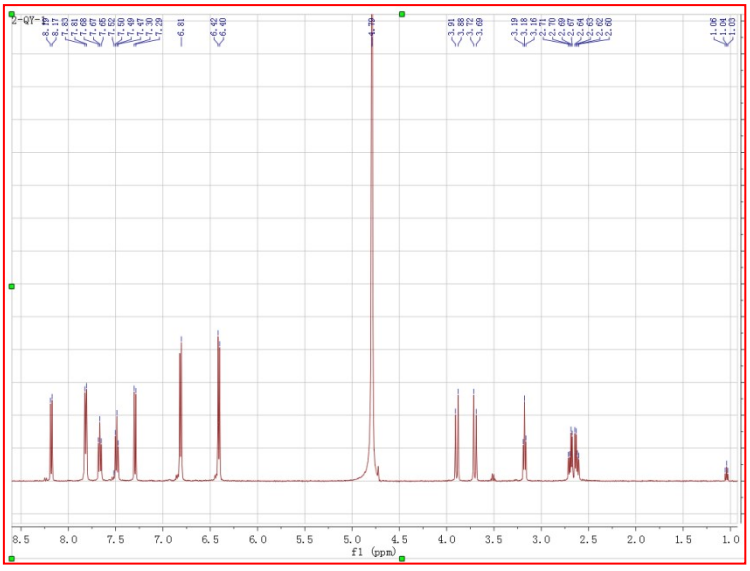

Fig. S3 ^{1}H NMR spectrum of 2-QY in D_2O.

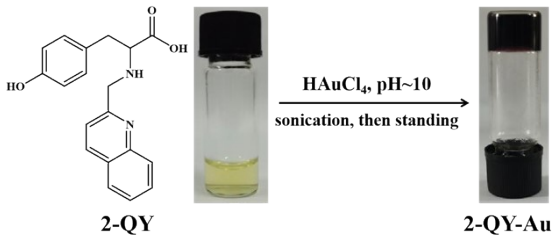

Fig. S4 The structure of 2-QY and the formation of 2-QY-Au NPs metallohydrogel.

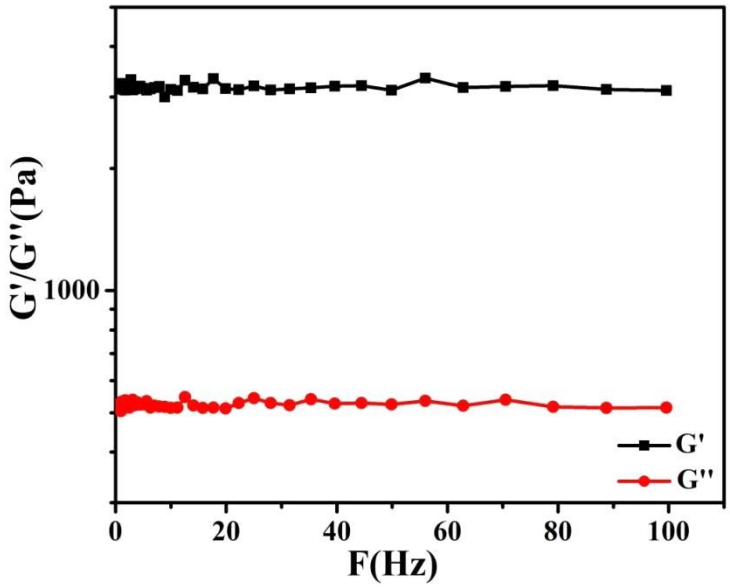

Fig. S5 The dynamic frequency scan of 2-QY-Au NPs metallohydrogel.

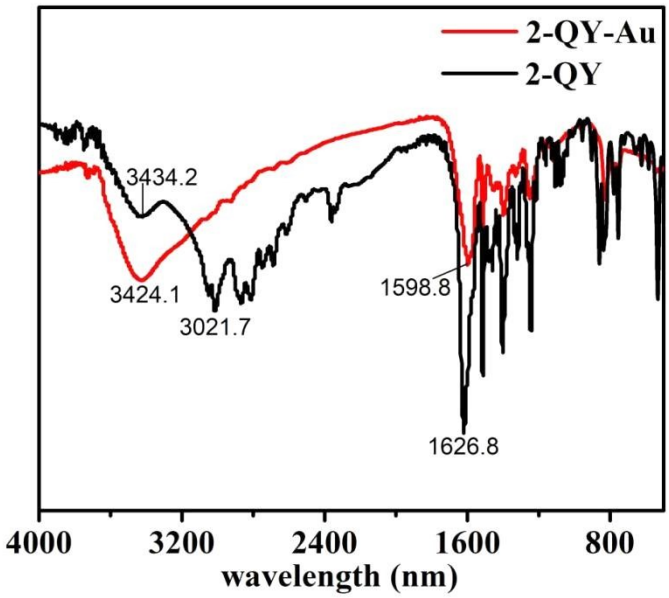

Fig. S6 The IR spectra of 2-QY powder and 2-QY-Au NPs xerogel.

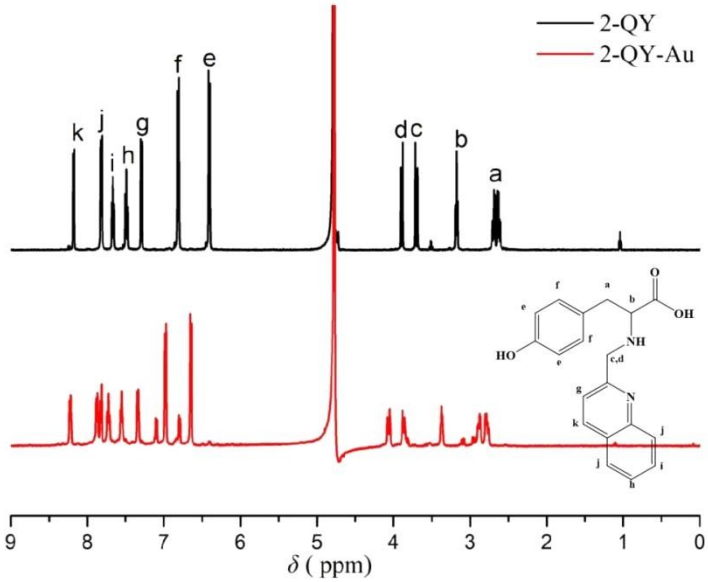

Fig. S7 ^{1}H NMR spectra of 2-QY and 2-QY-Au in D_2O.

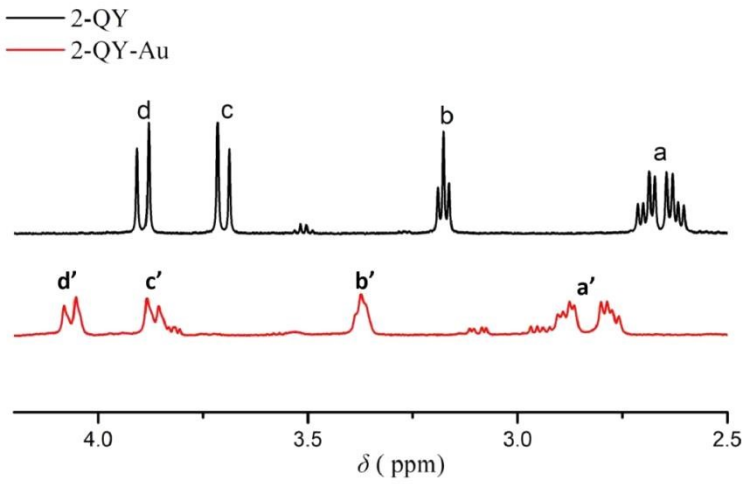

Fig. S8 ^{1}H NMR spectra of 2-QY and 2-QY-Au in D_2O (δ 4.2-2.5).

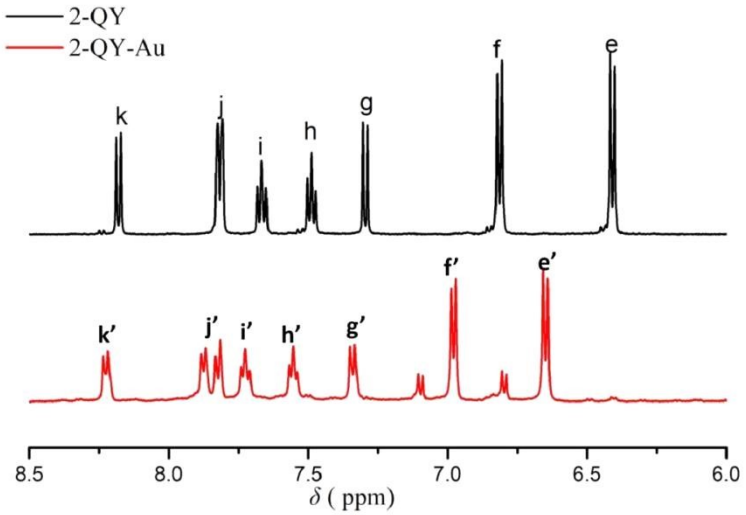

Fig. S9 ^{1}H NMR spectra of 2-QY and 2-QY-Au in D_2O (δ 8.5-6.0).

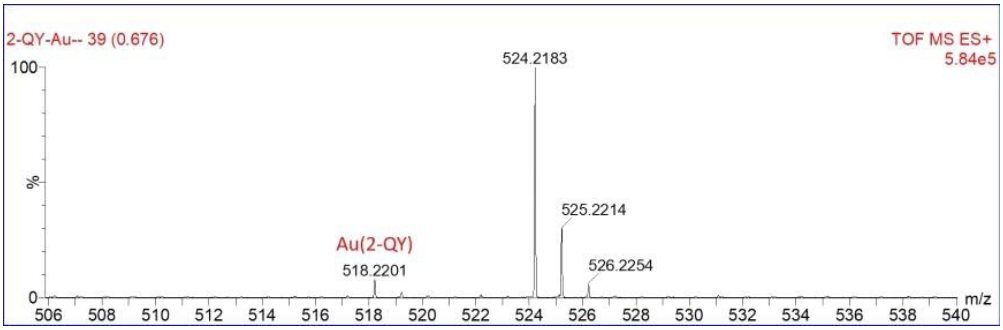

Fig. S10 ESI-MS spectra of 2-QY-Au complex, Calculated: 517.3 Da; Observed: 518.2 Da ([Au(2-QY) + H]).

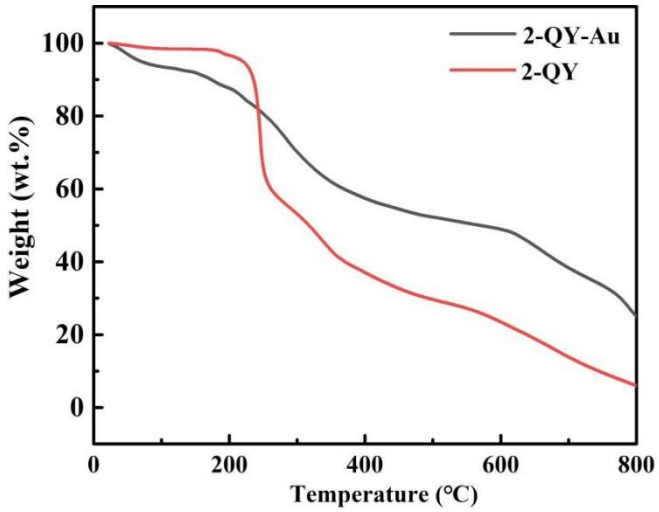

Fig. S11 Thermogravimetric analysis (TGA) thermogram of 2-QY powder and 2-QY-Au NPs metallohydrogel.

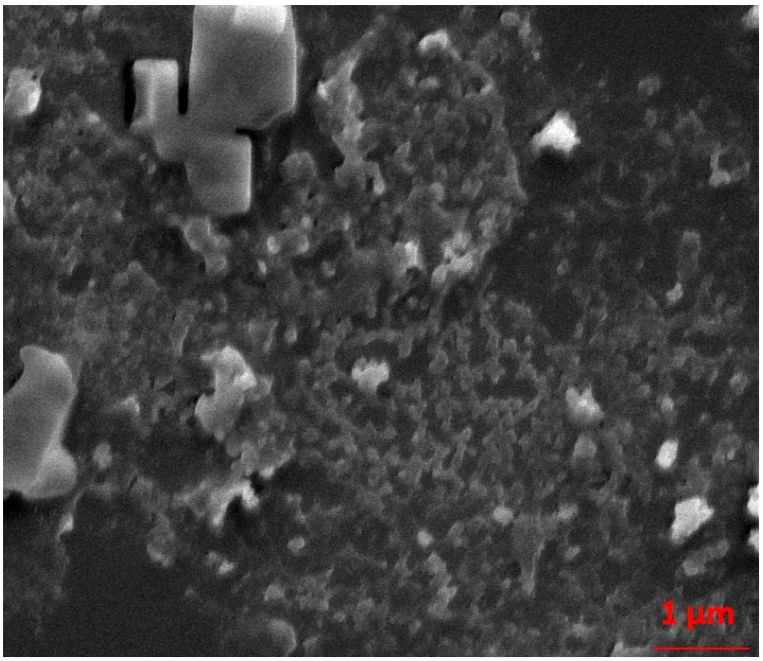

Fig. S12 SEM image of 2-QY solution.

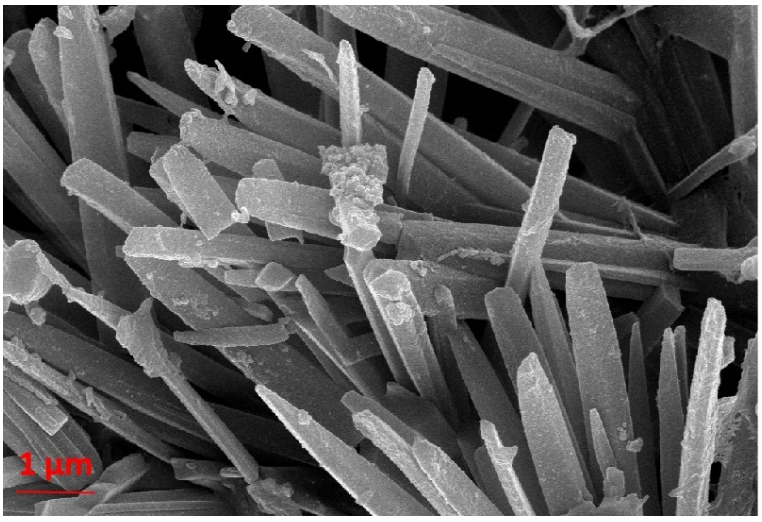

Fig. S13 SEM image of 2-QY-Au NPs xerogel.

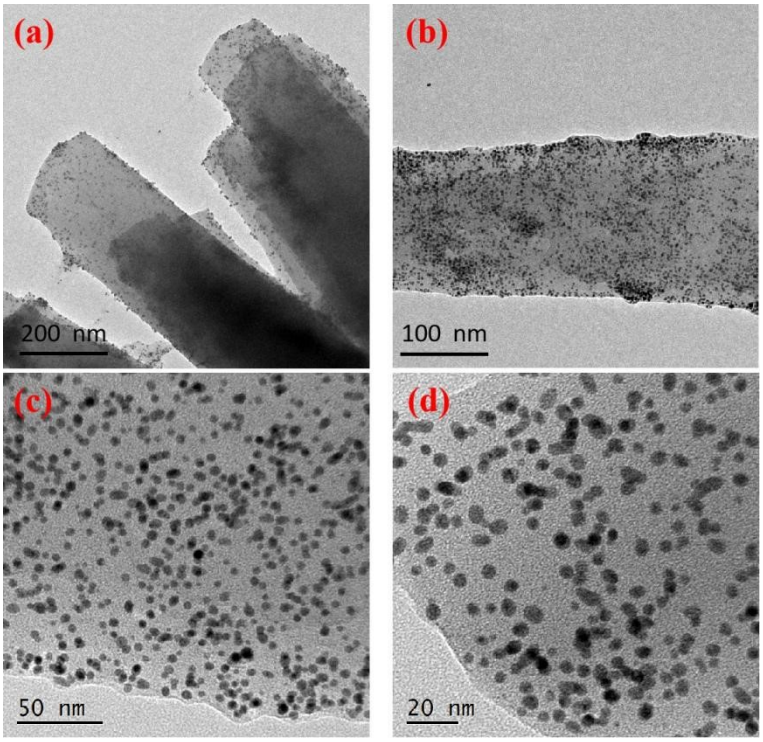

Fig. S14 TEM images of 2-QY-Au NPs xerogel at different scales (a) 200 nm, (b) 100 nm, (c) 50 nm, (d) 20 nm.

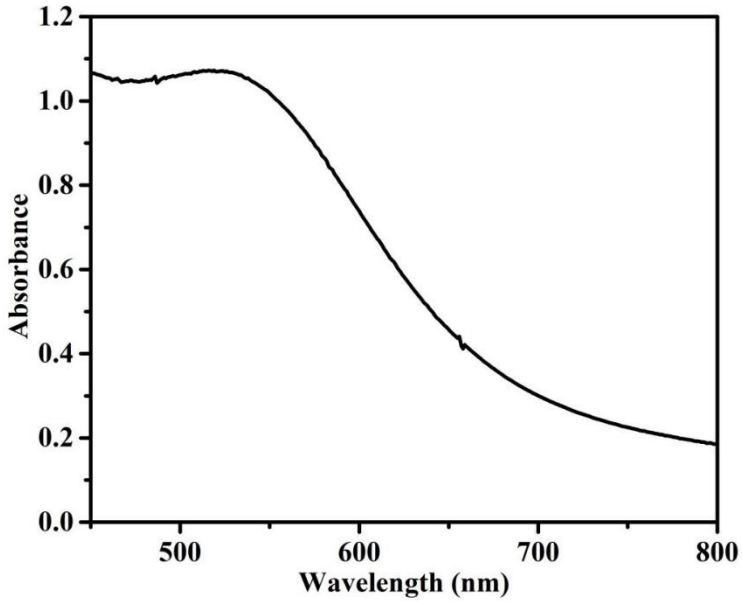

Fig. S15 UV-vis spectrum of the diluted 2-QY-Au metallohydrogel.

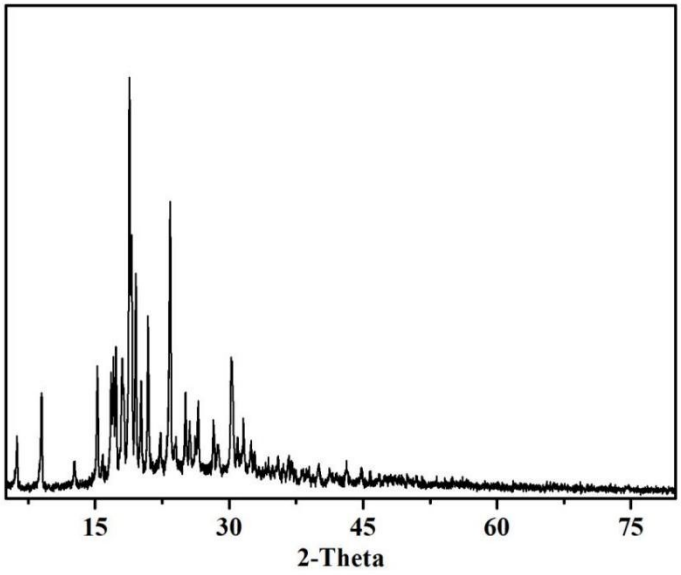

Fig. S16 XRD pattern of 2-QY powder.

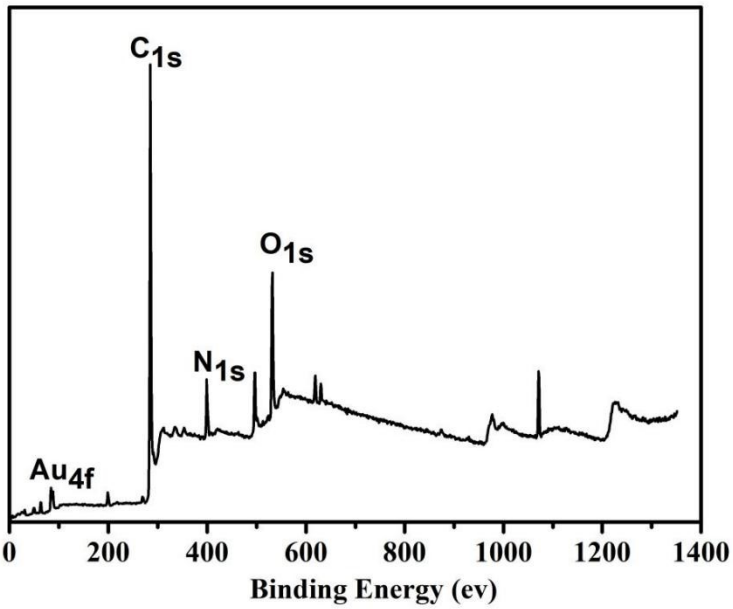

Fig. S17 X-Ray photoelectron spectroscopy of 2-QY-Au xerogel.

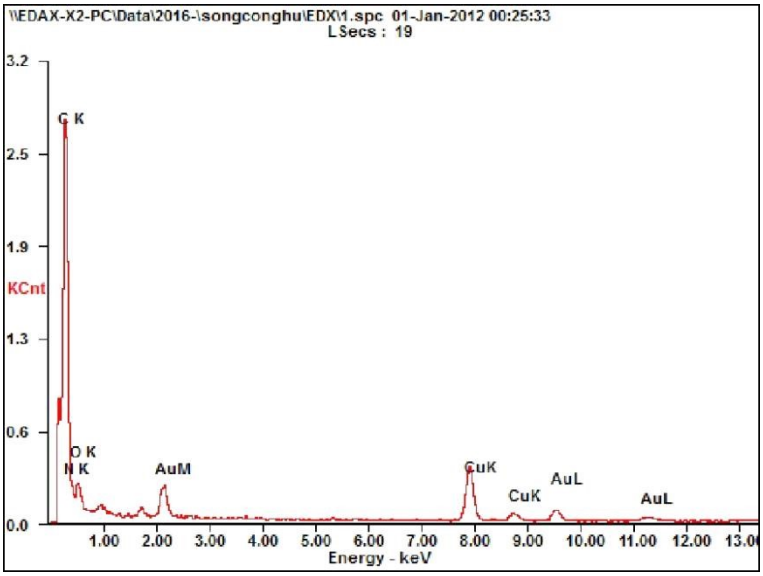

Fig. S18 EDX of 2-QY-Au NPs.

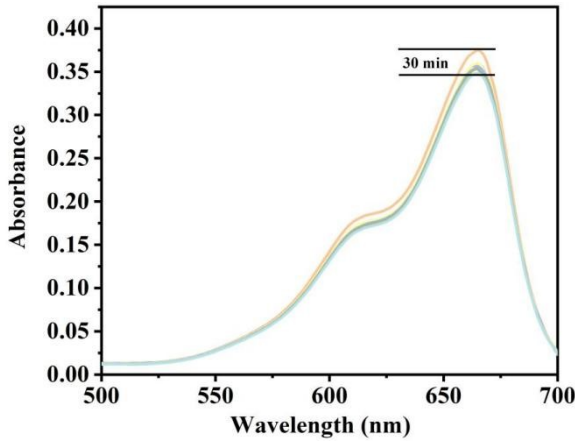

Fig. S19 Time-dependent UV-vis spectra of MB reduced by 2-QY without $NaBH_4$ and Au NPs. Reaction conditions: MB (10 μM), Au NPs (0.02 μM) and neutral pH.

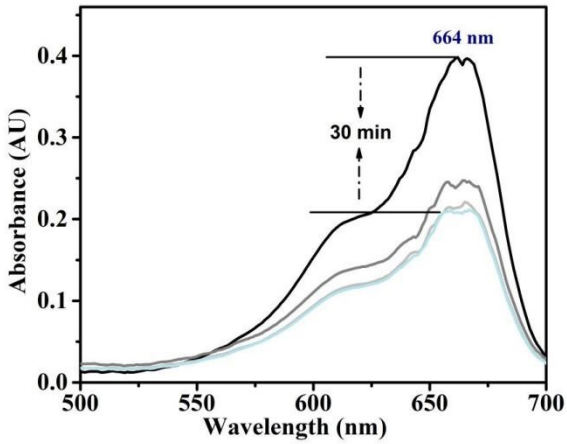

Fig. S20 Time-dependent UV-vis spectra of MB reduced by $NaBH_4$ in the presence of Au NPs prepared through $NaBH_4$ reduction. Reaction concentration: $NaBH_4$ (100 μM), MB (10 μM)，Au NPs (0.02 μM).

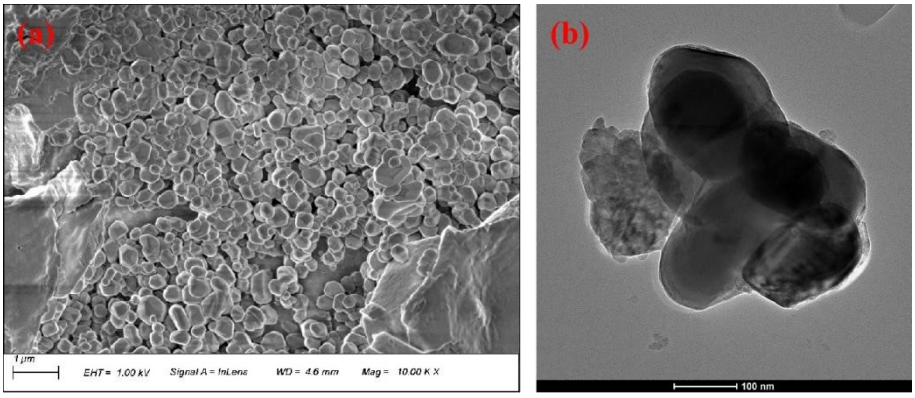

Fig. S21 SEM and TEM images of Au NPs prepared from $NaBH_4$ and $HAuCl_4$.

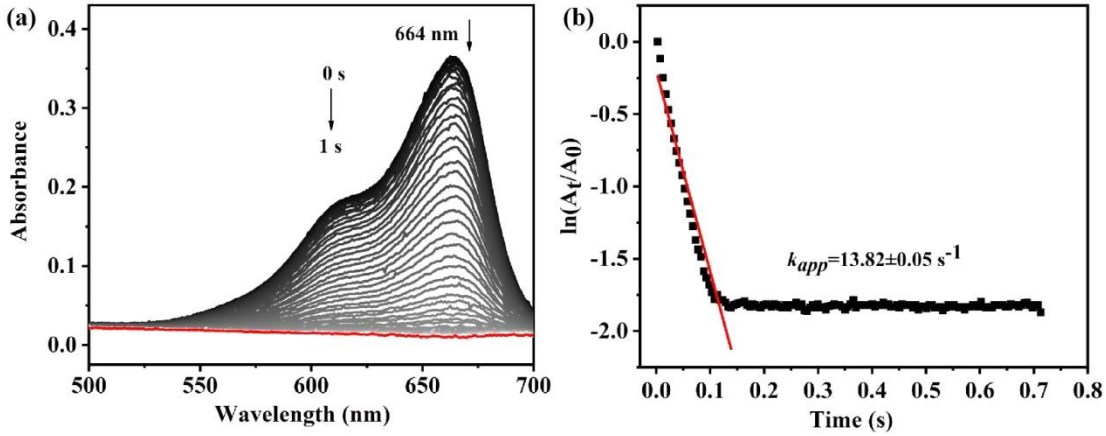

Fig. S22 Time-dependent UV-vis spectra of MB reduced by $NaBH_4$ (a) with 2-QY-Au NPs Xerogel, (b) the fitted curve of $\ln(A_t/A_0)$ versus reaction time for the degradation of MB with 2-QY-Au NPs metallohydrogel. Reaction conditions: initial MB concentration = 0.01 mM, $NaBH_4$ = 0.1 mM, catalyst dosage = 0.12 mg/mL, neutral pH, room temperature.

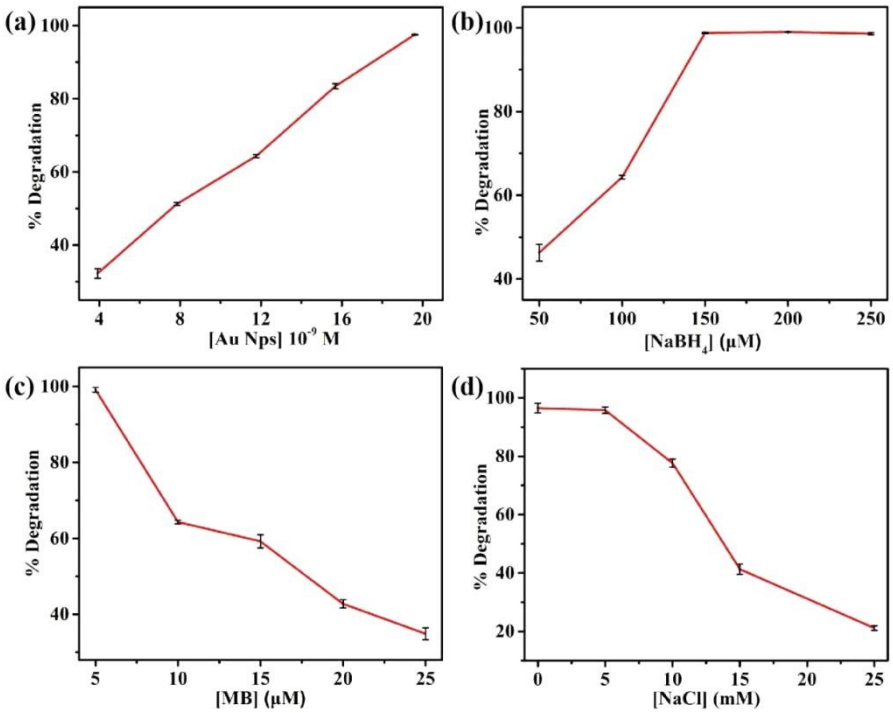

Fig. S23 The percentage of degradation of MB within 0.2 s at different effect factors (a) catalyst dose, (b) $NaBH_4$ concentration, (c) initial dye concentration, and (d) ionic strength. Reaction conditions: effect of catalyst dosage, [MB] = 0.01 mM, [$NaBH_4$] = 0.1 mM; effect of $NaBH_4$: [MB] = 0.01 mM, [Au NPs] =11.76×10^{-9} M; effect of initial dye concentration and effect ionic strength: [MB] = 0.01 mM, [Au NPs]=11.76×10^{-9} M.

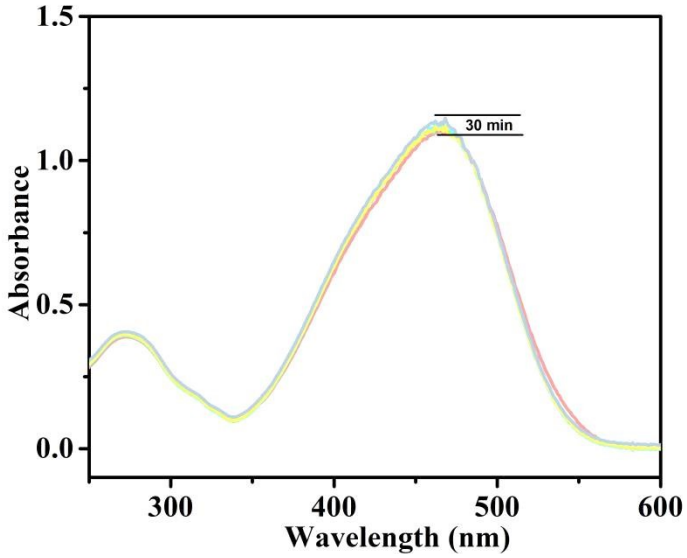

Fig. S24 Time-dependent UV-vis spectra of MO reduced by $NaBH_4$ without 2-QY-Au NPs metallohydrogel.

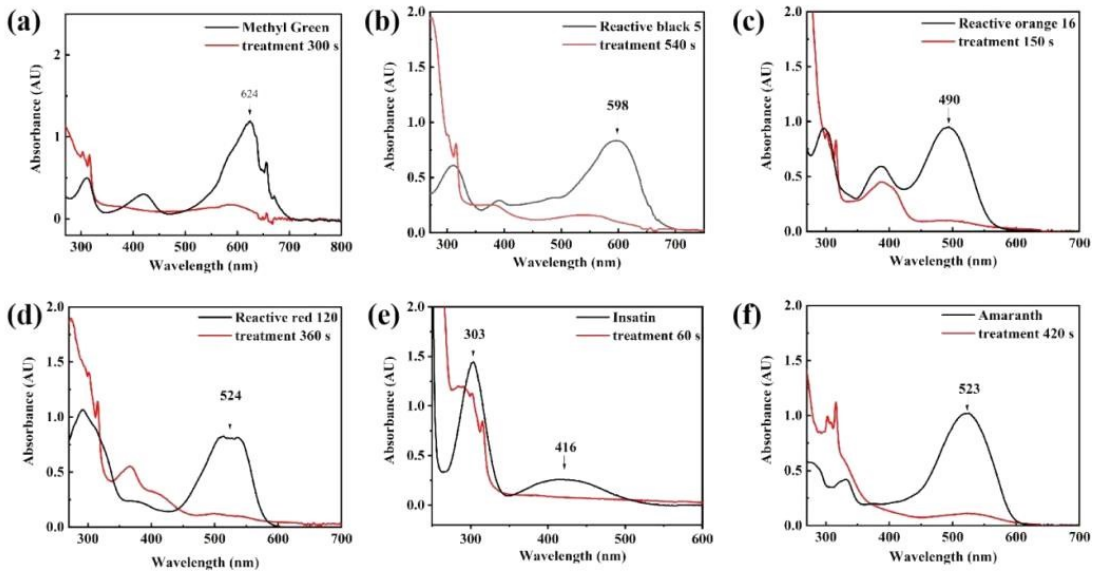

Fig. S25 UV-vis spectra of various dyes catalyzed by 2-QY-Au NPs (11.76×10^{-9} M): (a) Methyl green (50 μM) and $NaBH_4$ (100 μM), (b) Reactive black 5 (25 μM) and $NaBH_4$ (1 mM), (c) Reactive orange 16 (50 μM) and $NaBH_4$ (1 mM), (d) Reactive red 120 (25 μM) and $NaBH_4$ (5 mM), (e) Insatin (1 mM) and $NaBH_4$ (100 μM), (f) Amaranth (50 μM) and $NaBH_4$ (1 mM).

Table S1 The *kapp* and percentage of degradation of different dyes

Dyes	k_{app} (s^{-1})	Degradation percentage in 60 s
MB	13.1	99.23%
MO	0.21	98.75%
4-NP	0.013	42.53%
RB5	3.62×10^{-3}	27.75%
RO16	0.015	36.38%
RR120	5.15×10^{-3}	57.62%
instin	0.018	98.10%
Amaranth	4.55×10^{-3}	16.35%
MG	7.42×10^{-3}	60.51%

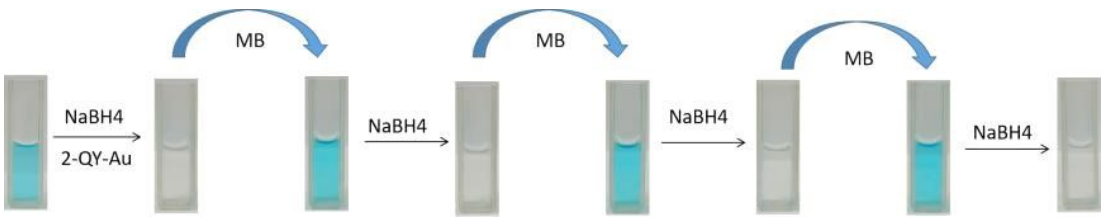

Fig. S26 Recycling photos of 2-QY-Au NPs metallohydrogel.

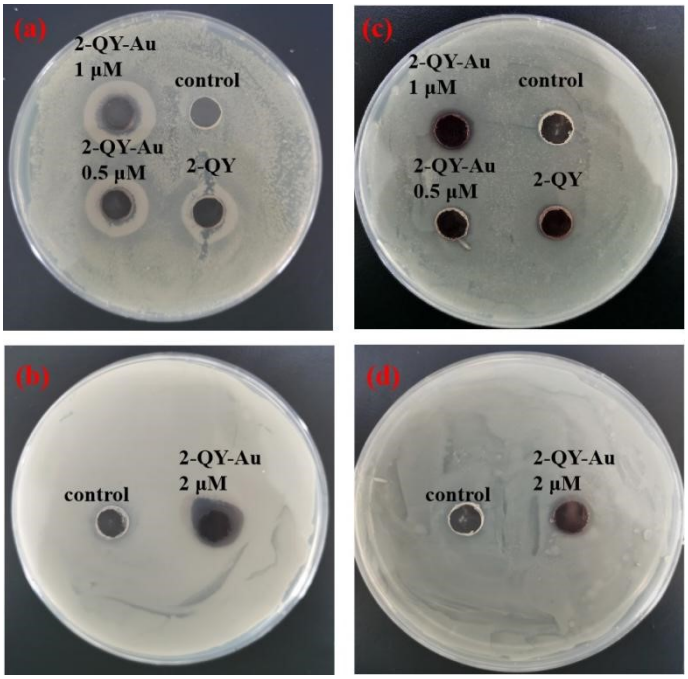

Fig. S27 The digital photos of colonies from (a, b) *B. subtilis*, and (c, d) *E. coli* treated without (control, 2-QY) and with diluted 2-QY-Au NPs gels under different concentrations.

Table S2. Inhibition effect of *E.coli* and *B. subtilis* under different concentrations of 2-QY-Au NPs gels.

		E.coli				*B.subtilis*			
Time (h)		6	12	18	24	6	12	18	24
2-QY-Au	0.5 μM	87.76%	67.89%	40.90%	42.26%	27.17%	15.14%	15.54%	14.90%
	1 μM	96.08%	96.73%	91.23%	84.96%	91.54%	80.99%	55.91%	52.29%
	2 μM	97.09%	96.19%	95.27%	91.65%	90.59%	93.46%	94.18%	97.68%

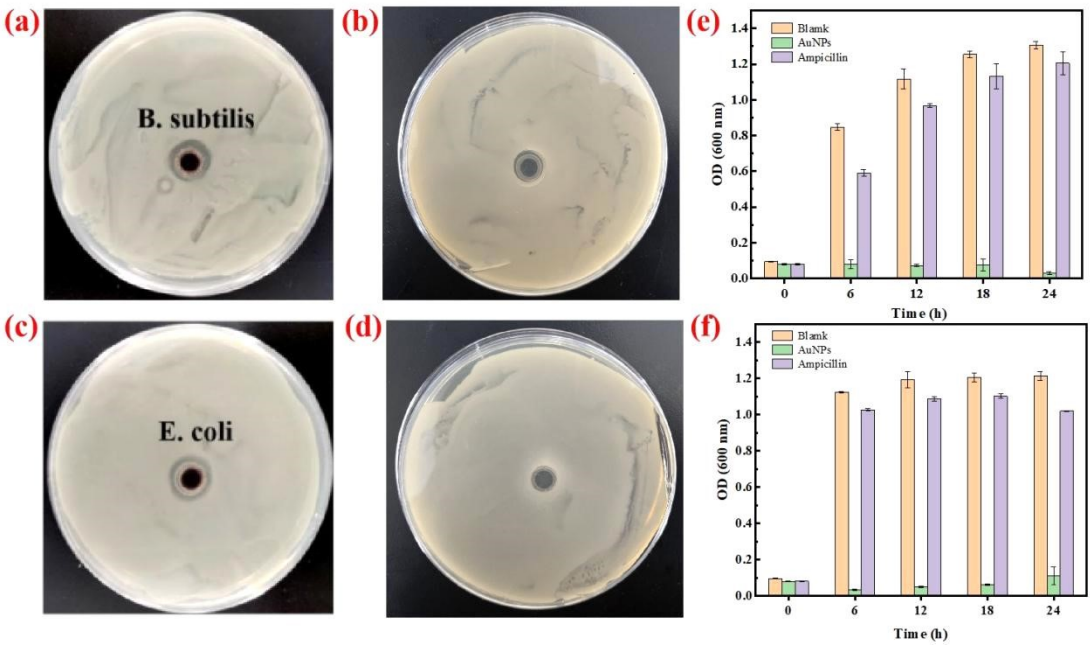

Fig. S28 The digital photos of colonies from (a, b) *B. subtilis*, and (c, d) *E. coli* treated with diluted 2-QY-Au NPs gels and ampicilin under 2 μM, respectively, Graphical representation of the OD measurements in (e) *B. subtilis*, (f) *E. coli* at different times (0 h, 6 h, 12 h, and 24 h, respectively).

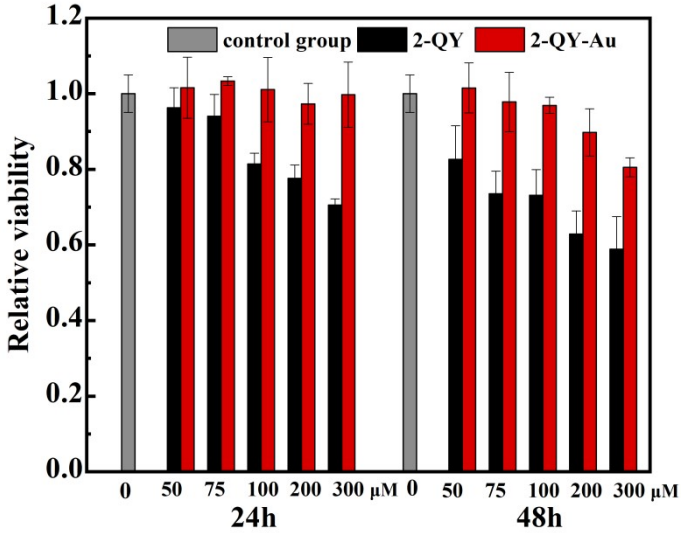

Fig. S29 MTT assays of 2-QY and 2-QY-Au NPs metallohydrogel. Error bars represent standard deviations from three repeated expected experiments.